KCI CONRETE JOURNAL
Vol.14 No.1, March 2002, pp.30-35

Crack Growth Behaviors of Cement Composites by Fractal Analysis

Jong-Pil Won[1)*] and Sung-Ae Kim [1)]

[1)] *Department of Rural Engineering Konkuk University, Seoul, Korea*

(This paper is English translation of the paper which has been awarded the 13th KCI paper of the year.)

Abstract

The fractal geometry is a non-Euclidean geometry which describes the naturally irregular or fragmented shapes, so that it can be applied to fracture behavior of materials to investigate the fracture process. Fractal curves have a characteristic that represents a self-similarity as an invariant based on the fractal dimension. This fractal geometry was applied to the crack growth of cementitious composites in order to correlate the fracture behavior to microstructures of cementitious composites. The purpose of this study was to find relationships between fractal dimensions and fracture energy. Fracture test was carried out in order to investigate the fracture behavior of plain and fiber reinforced cement composites. The load-CMOD curve and fracture energy of the beams were observed under the three point loading system. The crack profiles were obtained by the image processing system. Box counting method was used to determine the fractal dimension, D_f. It was known that the linear correlation exists between fractal dimension and fracture energy of the cement composites. The implications of the fractal nature for the crack growth behavior on the fracture energy, G_f is apparent.

Keywords: CMOD, cement composites, fractal dimension, fractal geometry, fracture energy

1. Introduction

Cement-based composites have two major deficiencies: low tensile strength and low energy consumption capacity, or toughness. One way to overcome these defects is to incorporate high-strength, small diameter fibers into the composite. The performance of the fiber-reinforced cement composites has shown a significant increase in the total energy consumption and overall toughness of the composites as compared to the plain matrix. In these cases, the fibers can provide sufficient bridging forces to suppress crack opening and redistribute the stresses to the nearby matrix, thus suppressing strain localization and creating multiple cracking.[10,12)] As fiber resists crack propagation, the crack curves. The crack growth behavior of matrix was very complex, because of the fiber. This is because the straight characteristic of the crack was obstructed by a reciprocal action between irregular structure and microcrack material and it twisted the crack shape, very unsteadily, resulting in a geometrically complex.[12)]

The crack growth behaviors of fiber reinforced cement composite are closely related to the fracture energy during the fracture process.[4,11)] However, in most existing studies, the crack is simply estimated by physical length and density, and not much effort went into the quantitative analysis of complex crack pattern. From this point of view, the application of fractal concept provides a useful method in the study of the quantitative analysis of highly irregular fracture surface and crack profiles.[1-8)]

Mandelbrot proposed the fractal concept in the 1970's and it is being applied to many natural phenomena these days. For example, it has been used to show the quantitative analysis of the crack pattern and the shape of fracture surfaces at the moment of a material fracture. The consuming fracture energy in fracture processing is related to the crack profiles of the fracture surface and physical property of the material as well. Therefore, the physical behavior in case of when cement composite fracture could be represented by a fractal characteristic of the fracture surface and crack shape. Irregular phenomena is expressed by a fractal curve, it describes property of space possession in each of place and possesses has property of differential impossibility.[1-4,7)]

In this study, fiber-reinforced cement composites were

* *Corresponding author*
Tel.: +82-2-450-3750; Fax.: +82-2-2201-0907
E-mail address: jpwon@konkuk.ac.kr

tested under three-point flexure, and the fracture energy was obtained from the experimental data. A complex crack pattern was quantified by fractal dimension. The complex crack pattern was formed because fiber suppresses cracks and resists crack propagation. Relationships between fracture energy and fractal dimension were analyzied.

2. Fractal geometry

2.1 Definition of fractal dimension

Mandelbrot proposed fractal dimension to overcome of limit of Euclidean geometry.[6] Generally, all the objects studied in mathematics or physics are continuous, linear and smooth, but nature shows us that such is not always the case. Natural objects are generally rough and discontinuous.

By definition, and inherent property of fractal objects is the statistical replication of patterns at different scales; a magnified part of a fractal object is statistically identical to the whole shape. This property can be fractal dimension. The fractal dimension D_f is defined as equation (1).[3]

$$N = r^{D_f} \tag{1}$$

Where, N is number of subpart, r is scaling factor, which is inverse of number of the whole length divided by unit length r. As both side of Equation (1) take logarithm, fractal dimension, D_f is following.

$$D_f = \frac{\ln N}{\ln r} \tag{2}$$

Fig. 1 illustrates the generation of a self-similar synthetic fractal curve the triadic Koch curve. First, an initiator is defined. It represents an initial geometric form, and then a generator, which describes a transformation on the initiator, is applied.

As the transformation operation is repeatedly applied to the figure, a fractal curve is generated. For the triadic Koch curve, we note that at each step the number of line segments increased to four factors and that the length of each new line segment generated is one-third of the previous segment length at each step. At the step, $\eta = 2$, the number of subdivisions N is 16; the scaling factor, r is 9; fractal dimension is estimated as equation (3).

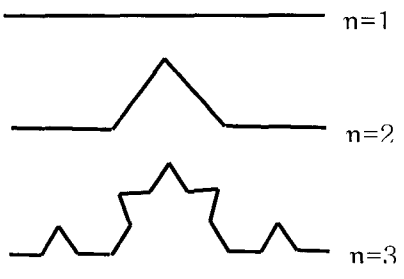

Fig. 1 Stages in generation of the triadic Koch curve

$$D_f = \frac{\ln 16}{\ln 9} \tag{3}$$

Therefore, fractal dimension of Koch curve is 1.2619, if the transformation operation were infinite repeated.

2.2 Correlation between fractal dimension and fracture energy

According to Richardson, the relationship between the scale of the measurement and that of actual measurement that can be presented by fractal dimension was following equation (4).[4,9]

$$L(\eta) = L_0 \eta^{1-D_f} \tag{4}$$

Where, D_f is the fractal dimension, L_o is the length of the crack when $D_f=1$, which means the crack path is a straight line, ε_i is the scale of the measurement with no dimension. The front of fractal equation means that the actual length in the natural situation can be shown at a different value according to the scale of measurement. As this equation applied to the crack profile, which formed during the fracture process of the material, it is expressed by the ratio of the crack length of measurement to straight crack path. This equation was applied to crack growth behaviors, fractal crack length, a_f can be showed as following equation.[9]

$$a_f = a_0^{D_f} \varepsilon^{1-D_f} \tag{5}$$

where, $\varepsilon = \eta \cdot a_o$

Critical energy release rate, G_{IC} is following (6)

$$G_{IC} = \frac{\partial U_e}{\partial(2a)} = \frac{\partial U_s}{\partial(2a)} = \frac{\pi\sigma^2}{E} \tag{6}$$

Where, *Ue* is elastic energy, *Us* is crack growth energy. Fractal crack length of equation (5) was inserted to equation (6), and following equation was obtained (7).

$$G_{IC} = \frac{\pi\sigma^2}{E} a_0^{D_f} \varepsilon^{1-D_f} = 2\gamma \quad (7)$$

Where, γ is surface energy.

3. Fracture test

3.1 Materials and mix proportions

Materials used in this experimental study were Type I cement (specific gravity: 3.15) and sand (specific gravity: 2.60). A melamin based water-reducing AE agent was used to maintain certain limits of flow in the cement composites.

Physical properties of cement and sand are given in Table 1 and 2. The properties of cellulose and polypropylene fibers are given in Table 3.

The cement matrixes were used with and without fibers varying volume fractions. Target compressive strength for a plain mortar was 270±5kgf/cm^2, flow value was 220±5mm, and air was 27%.

Two different fibers, polypropylene and cellulose, were investigated at several volume fractions. The mixture proportions are given in Table 4.

3.2 Preparations of test specimens

Prism specimen (30x60x240mm) was made for static three point flexural tests. An average of four specimens for each mixture was selected for two different batches. After curing for 24 hours, specimens were demolded and cured in water of 22±3℃ until tested at the total age of 28days from manufacture. A deep notch was cut into the specimen in the middle cross section to enable measurement of the crack mouth opening displacement (CMOD) and to control the stable test. The scheme of the test is illustrated in Fig. 2.

3.3 Test equipment and test methods

A static three-point flexural test was done using a displacement control universal test machine. The crosshead speed was maintained 0.1mm/mim. Both of the initial notches were fitted with a crack gage in order to measure CMOD. For maximum contrast in the images, a white paint was used at the expected place of crack propagation.

Test results were obtained using automatic data acquisition and image processing equipment. Load-CMOD curves were obtained. CMOD was measured up to about 0.4mm. Flexural strength and fracture energy were computed by equation (8) and (9).

$$f_b = \frac{3P_{max}\, l}{2b(h-a)^2} \quad (8)$$

Whereas, f_b: flexural strength
P_{max}: maximum load
L: span, b: width
h: depth, a: notch length

Table 1 Physical properties of cement

Fineness (cm^2/g)	Specific gravity	Stability (%)	Compressive strength (kgf/cm^2)		
			3 days	7 days	28 days
3,488	3.15	0.08	224	308	404

Table 2 Physical properties of fine aggregate

Specific gravity			Absorption(%)	F.M.
Bulk	Bulk(SSD)	Apparent		
2.57	2.59	2.63	0.67	2.99

Table 3 Properties of special cellulose and polypropylene fibers

Property	Fiber type	
	Cellulose fiber	Polypropylene fiber
Elastic modulus(kgf/cm^2)	61×10^4	3.5×10^4
Bond strength(kgf/cm^2)	15.3	4.1
Specific gravity	1.5	0.9
Fiber length(mm)	2.92	10
Effective diameter(mm)	0.015	0.1
Aspect ratio	200	190
Tensile strength(kgf/cm^2)	5100	6210
No. of fiber per gram	1,100,000	12000
Fiber count, 1/cm^3	1430	0.6
Specific surface(1/cm)	0.13	0.033

Table 4 Mix proportions

Type	Cement (kg/m^3)	Water (kg/m^3)	Sand (kg/m^3)	Fiber volume fraction (%)	Superplasticizer with air entrained admixture(kg/m^3)
Plain	477.2	295.9	1431.6	-	4.7
Polypropy -lene fiber	477.2	295.9	1431.6	0.10	4.7
Cellulose fiber	477.2	295.9	1431.6	0.06	4.7
	477.2	295.9	1431.6	0.08	4.7
	477.2	295.9	1431.6	0.10	4.7
	477.2	295.9	1431.6	0.13	4.7

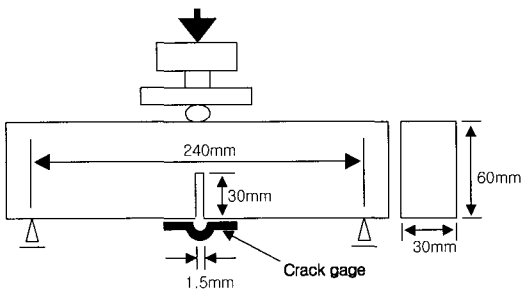

Fig. 2 The schematic diagram of test apparatus

$$G_f = \frac{A}{b(h-a)} \quad (9)$$

Whereas, G_f : fracture energy
A : area of under load-CMOD curve
b : width
a : notch length
h-a : crack growth length

4. Fractal analysis

4.1 Image processing and crack recognition

After fracture test, in order to retrieve more detailed information regarding the cracks that developed on the surface of the specimen, image was recorded with Sony DSC-F505K system with high-resolution. It was equipped with both 5 magnifications and 2,110,000 pixels. The digital camera was at a distance of 100mm from the specimen surface. In order to extract the topological information on the image patterns, starting from the complex image (Fig. 3(a)), thresholding has proven to be the most effective routine (Fig. 3(b)). Crack propagation paths were recognized through filtering of the images that removed unnecessary part (Fig. 3(c)). This method is simple; a sequence of grids, each of which, having a different cell size, is placed over maps of the crack shapes and then the number of cells intersected by crack shapes are counted. The number of grid cells intersected by the profile N , and then plotted on a log-log scale with respect to the inverse of the grid cell size. This relationship was shown equation (10)

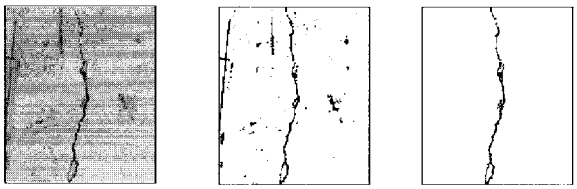

(a) Original Image (b) Thresholding (c) Filtering

Fig. 3 Image processing on a crack patterns

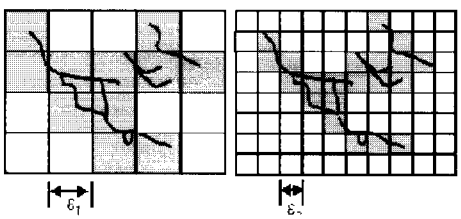

Fig. 4 Box counting method

$$N = \left(\frac{1}{\varepsilon}\right)^{D_f} \quad (10)$$

This graph taken the slope of linear growth of the number of cells against the inverse of the grid cell size, as power law. In the relationship, an exponent is the slope of straight line, and that is fractal dimension.

The fractal dimension exceeds the Euclidean dimension. Dimension will take the place for a curve between D_f=1(smooth line) and D_f=2(Euclidean dimension of surfaces). D_f=1~2(fractal curve).

Following equation (11) shows fractal dimension.

$$D_f = \frac{\ln(N)}{\ln(1/\varepsilon)} \quad (11)$$

5. Test results and research

5.1 Flexural strength and fracture energy

Table 6 shows the results of flexural strength and fracture energy in plain mortar and fiber reinforced mortar with polypropylene fiber volume fraction of 0.1%, and with cellulose fiber volume fraction of 0.06~0.13%.

Fig. 5 shows the typical Load-CMOD curve in the fracture tests. Plain mortar failed suddenly once the CMOD corresponding to the ultimate flexural strength was exceeded. On the other hand, fiber reinforced cement composites continuous to sustain considerable loads even at the displacement of considerable excess of the fracture displacement of the plain mortar. Therefore, in the fiber-reinforced cement composites, fiber contributed to the enhancement of the strength and crack resistance property and a sharp rise in the energy absorption of the material occurs. To speak more precisely, it contributed much more to the energy absorption of composite than to the strength.

Based on the results of the flexural test shown in fig. 5, the load carring capacity of 0.1% fiber volume fraction of polypropylene were 1.27% times better than that of plain mortar, and for those of 0.06%, 0.08%, 0.1%, 0.13% fiber volume fractions of cellulose were 1.16, 1.40, 1.20, and 1.10 times better than that of plain mortar.

The fracture energy can be obtained from the area under the load-CMOD curve in the flexure shown in Fig. 6. The fracture energy of 0.1% polypropylene fiber case and 0.06%, 0.08%, 0.1%, 0.13% fiber volume fraction of cellulose fiber reinforced cement composite cases were 1.96, 1.61, 2.04, 1.96, and 1.57 times better than that of plain mortar. These results were caused by fiber fracture, bridging crack, and fiber-matrix debonding which showed

Table 6 Fracture test results

matrix		a/H	Curing Age (days)	σ_u (kgf/cm^2)		G_f ($\times 10^{-2}$kgf/cm)	
Plain		0.5	28	25.97 21.51 26.23	mean 24.57	2.74 2.79 3.33	mean 2.95
PP(0.1%)		0.5	28	29.27 32.43 31.92	mean 31.21	5.63 5.97 5.69	mean 5.76
Cellulose	0.06%	0.5	28	29.55 31.10 27.21	mean 28.65	4.77 4.83 4.65	mean 4.75
	0.08%	0.5	28	34.80 35.83 32.29	mean 34.31	5.85 6.28 5.96	mean 6.03
	0.1%	0.5	28	26.95 29.29 31.87	mean 29.37	5.68 5.89 5.77	mean 5.78
	0.13%	0.5	28	26.76 26.69 26.79	mean 26.75	4.64 4.53 4.70	mean 4.62

that added fiber contributed to softening behavior of the composite.

5.2 Relationship between fractal dimension and fracture energy

In this study, after the fracture test of cement composites, fractal analysis was carried out about crack pattern on the fracture surface. Fig. 8 showed the results of fractal dimension in different types and volume fractions of fiber. The results showed that the fractal dimension of fiber-reinforced cement composites was higher than that of plain mortar. The range of fractal dimension was 0.992~1.036. Relationship between fracture energy and fractal dimension of cement composites is presented in Fig. 9. Fig. 8 showed that fracture energy was increased as the fractal dimension of the crack profile was increased, and a linear correlation was observed.

This results were caused by the softening behavior during the fracture process of fiber reinforce composites. The fiber provide bridging forces to suppress crack opening, so the crack resistance forces were increased.

The fibers can increase crack resistance force. Also, crack was obstructed by reciprocal action between irregular structure and microcracks of material, and it makes the crack shape be twisted very unsteadily and geometrically complex.

Therefore, the fractal dimension can be used for the quantitative analysis of fracture energy and predict crack growth behavior, which describes complex characteristic of crack patterns.

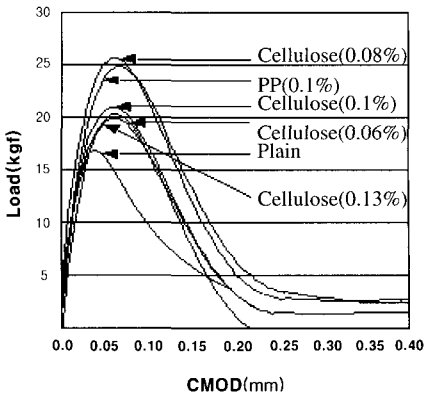

Fig. 5 Typical Load-CMOD curve of cement composites

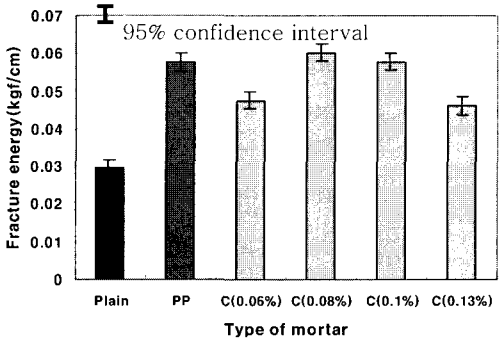

Fig. 6 Fracture energy of cement composites

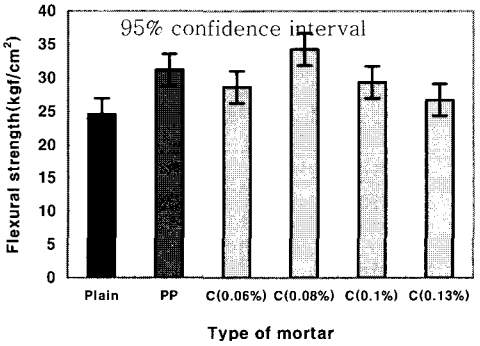

Fig. 7 Flexural strength of cement composites

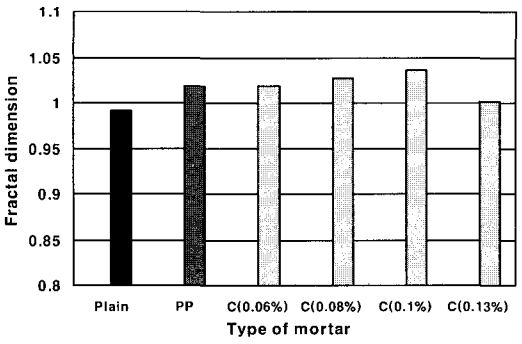

Fig. 8 Fractal dimension of cement composites

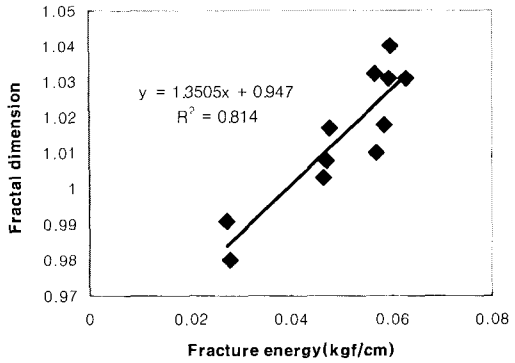

Fig.9 Correlation between fractal dimension and fracture energy of cement composites

6. Conclusions

Fracture test was carried out in order to investigate the fracture behavior of plain and fiber reinforced cement composites. The load-CMOD curve and fracture energy of the beams were obtained under the three point loading system. The crack profiles were obtained by the image processing system. Box counting method was used to determine the fractal dimension, D_f. The relationships between fractal dimension and fracture energy of cement composites are as follows.

1) The fractal dimensions of fiber reinforced cement composites obtained using different types and volume fractions of fibers ranged between 0.992 and 1.036. In addition, fractal dimensions were generally increased as the fracture energy of composite was increased, as positive correlation was demonstrated.
2) Fractal dimension can be the quantitative analysis of fracture energy and prediction of crack growth behavior, which describes complex characteristic of crack patterns.

REFERENCES

1. Kwon, O.H. and Goo, D.H., "Fractal characteristic analysis Applied to fracture parameter," *Journal of KISS*, Vol.13, No.4, 1998, pp. 71-78.
2. Kwon, O.H. and Youn, Y.S., "The study of evaluation for high toughness crack behaviors," *Journal of Pukyong National University*, Vol.3, No.2, pp. 155-162.
3. Cho, S.S. and Joo, W.S., "A Study on self-similarity of materials damage using fractal dimension," *Journal of Donga University*, Vol.4, No.1, 1999, pp. 7-15.
4. Jeon, C. H. Kwun, S. Z., and Shin, M. C., "The fractal analysis of material," *Journal of the Korea Institute of Metals and Materials*, Vol.33, No.2, pp. 276-279.
5. Carpinteri, A. and Chiaia, B., "Multifractal scaling law for the fracture energy variation of concrete structure," *Fracture Mechanics of Concrete Structure*, Proceedings FRAMCOS-2, 1995, pp. 581~596.
6. Mandelbrot, .B.B., "*The fractal geometry of nature*," W. H. Freeman and Co., New York, 1982.
7. Lange, David A., Hamlin, M. Jennings, and Shah, Surendra P., "Relationship between fracture surface roughness and fracture behavior of cement paste and mortar," *Journal of American Ceramic Society*, Vol.76, No3, 1993, pp. 589~597.
8. Saouma, Victor E. and Barton, Christopher C., " Fractals, fractures and size effects in concrete," Journal of Engineering Mechanics, Vol.20, No4, April, 1994, pp835~854.
9. Bazant, Zdenek P. and Planas, Jaime, "*Fracture and size effect in concrete and other quasibrittle materials*," CRC Press, 1998, pp480~487.
10. Li, Zongijn, Li, Faming, Chang, T.Y. Paul, and Mai Y.W., "Uniaxial tensile behavior of concrete reinfoced with randomly distributed short fibers," *ACI. Material Journal*, 95, 1998.
11. Mandelbrot, B.B. and Freeman, W. H., "*Fiber reinforced cementitious composites*," San Francisco, CA, 1992.
12. Arnon Bentur, *Sidey Mindess*, ELSEVIER SCIENCE PUBLISHERS LTD, 1990.